3

Negative Refractive Index Composite Metamaterials for Microwave Technology

Nicola Bowler
Iowa State University
USA

1. Introduction

Materials that exhibit negative index (NI) of refraction have several potential applications in microwave technology. Examples include enhanced transmission line capability, power enhancement/size reduction in antenna applications and, in the field of nondestructive testing, improved sensitivity of patch sensors and detection of sub-wavelength defects in dielectrics by utilizing a NI superlens.

Since NI materials do not occur naturally, several approaches exist for creating NI behaviour artificially, by combinations of elements with certain properties that together yield negative refractive index over a certain frequency band. Present realizations of NI materials often employ metallic elements operating below the plasma frequency to provide negative permittivity ($\varepsilon < 0$), in combination with a resonator (e.g. a split-ring resonator) that provides negative permeability ($\mu < 0$) near resonance. The high dielectric loss exhibited by metals can severely dampen the desired NI effect. Metallic metamaterials also commonly rely on periodic arrays of the elements, posing a challenge in fabrication. A different approach is to employ purely dielectric materials to obtain NI behaviour by, for example, relying on resonant modes in dielectric resonators to provide $\varepsilon < 0$ and $\mu < 0$ near resonance. Then, the challenge is to design a metamaterial such that the frequency bands in which both ε and μ are negative overlap, giving NI behaviour in that band. Two potential advantages to this approach compared with NI materials based on metallic elements are i) decreased losses and ii) simplified fabrication processes since the NI effect does not necessarily rely on periodic arrangement of the elements.

This chapter explains the physics underlying the design of purely dielectric NI metamaterials and will discuss some ways in which these materials may be used to enhance various microwave technologies.

2. Basic Theory of Left-Handed Light

2.1 Effective permittivity and permeability of a composite material

In this chapter, the design of materials with negative refractive index, $n < 0$, will proceed on the basis of achieving negative real parts of effective permittivity, ε, and permeability, μ, in a

composite material. Such a material is termed 'double-negative' or 'DNG'. First, let's discuss what is meant by *effective* parameters ε and μ.
Adopting notation in which the vector fields are denoted by bold font and second-order tensors by a double overline, the constitutive relations can be written as

$$\boldsymbol{D} = \bar{\bar{\varepsilon}} \cdot \boldsymbol{E} \quad \text{and} \quad \boldsymbol{B} = \bar{\bar{\mu}} \cdot \boldsymbol{H}, \tag{1}$$

in which $\boldsymbol{D}$ is electric displacement, $\boldsymbol{E}$ is the electric field, $\boldsymbol{B}$ is the magnetic induction field and $\boldsymbol{H}$ is the magnetic field. In the following development, however, it will be assumed that the materials are isotropic so that ε and μ are scalar. Then,

$$\boldsymbol{D} = \varepsilon \boldsymbol{E} \quad \text{and} \quad \boldsymbol{B} = \mu \boldsymbol{H}. \tag{2}$$

The assumption of isotropic properties holds for cubic lattices and entirely random structures of spherical particles embedded in a matrix, for example.
It is often convenient to work in terms of dimensionless relative permittivity and permeability, ε_r and μ_r , respectively, which are related to ε and μ by the free-space values $\varepsilon_0 = 8.854 \times 10^{-12}$ F/m and $\mu_0 = 4\pi \times 10^{-7}$ H/m as follows;

$$\varepsilon = \varepsilon_r \varepsilon_0 \quad \text{and} \quad \mu = \mu_r \mu_0. \tag{3}$$

2.2 Double-negative means negative refractive index

Considering the following familiar definition of the refractive index,

$$n = \sqrt{\varepsilon_r \mu_r}, \tag{4}$$

it is not immediately obvious why, in the case of a double-negative (DNG) medium, with $\mathrm{Re}\{\varepsilon\} < 0$ and $\mathrm{Re}\{\mu\} < 0$ that $n < 0$ as well. The answer lies in the fact that ε_r, μ_r and n are, in general, complex quantities. Practically speaking, ε_r and μ_r exhibit complex behaviour at frequencies close to a resonance or relaxation. These kinds of processes exist at microwave frequencies in many materials and some of them will be discussed in following sections of this chapter. So, given that ε_r and μ_r may be complex, write

$$\varepsilon_r = |\varepsilon_r| e^{-j\theta} \quad \text{and} \quad \mu_r = |\mu_r| e^{-j\phi}, \tag{5}$$

where it is assumed that fields are varying time-harmonically as $\mathrm{Re}\{e^{j\omega t}\}$ with $\omega = 2\pi f$ the angular frequency and f the frequency in Hz. Then, from (4),

$$n = \sqrt{|\varepsilon_r||\mu_r|} e^{\pm j(\theta+\phi)/2}. \tag{6}$$

From (6) it is clear that in order to determine the sign of n when $\mathrm{Re}\{\varepsilon\} < 0$ and $\mathrm{Re}\{\mu\} < 0$, the phase angles θ and ϕ must be considered.

Notice, first, that if $\mathrm{Re}\{\varepsilon\} < 0$ and $\mathrm{Re}\{\mu\} < 0$ then both θ and ϕ lie between the limits $\pi/2$ and $3\pi/2$. [This can be shown by employing Euler's theorem $e^{-j\psi} = \cos\psi - j\sin\psi$ and considering the properties of the cosine function.] This also means that

$$\frac{\pi}{2} < \frac{\theta + \phi}{2} < \frac{3\pi}{2}. \tag{7}$$

Secondly, the condition that is required for the medium to be passive, or non-absorbing, will be applied. This has the effect of further restricting the range of $(\theta + \phi)/2$. In the case of a

passive medium, $\mathrm{Im}\{n\} < 0$. Again from Euler's theorem but now considering the properties of the sine function, the restriction that the imaginary part of n is negative and taking the appropriate root from (6) leads to the condition

$$0 < \frac{\theta + \phi}{2} < \pi. \tag{8}$$

Finally it can be seen that satisfaction of both (7) and (8) requires

$$\frac{\pi}{2} < \frac{\theta + \phi}{2} < \pi \tag{9}$$

and, due to the fact that $\cos[(\theta + \phi)/2] < 0$ when (9) applies, it follows that

$$\mathrm{Re}\{n\} = \sqrt{|\varepsilon_r||\mu_r|}\cos[(\theta + \phi)/2] < 0 \tag{10}$$

for a passive medium in which $\mathrm{Re}\{\varepsilon\} < 0$ and $\mathrm{Re}\{\mu\} < 0$.

In contrast with the refractive index, the impedance of a medium, defined

$$Z = \sqrt{\frac{\mu_r \mu_0}{\varepsilon_r \varepsilon_0}}, \tag{11}$$

retains its positive sign in a DNG medium (Caloz et al., 2001; Ziolkowski & Heyman, 2001).

2.3 Wave propagation in a negative-refractive-index medium

We have shown that a double-negative medium has a negative index of refraction. What consequences follow for the propagation of an electromagnetic wave in such a medium?

A negative-refractive-index medium supports *backward wave propagation* described by a left-handed vector triad of the electric field $\boldsymbol{E}$, magnetic field $\boldsymbol{H}$, and wave vector $\boldsymbol{k}$ (Veselago, 1968; Caloz et al., 2001). Both $\boldsymbol{k}$ and the phase velocity vector $\boldsymbol{v}_p$ exhibit a sign opposite to that which they possess in a conventional right-handed medium (RHM). This has led to such materials also being known as left-handed materials (LHMs), but it should be noted that left-handedness is not a necessary nor sufficient condition for negative refraction (Zhang & Mascarenhas, 2007). Regarding the Poynting vector $\boldsymbol{S}$ and the group velocity $\boldsymbol{v}_g$ in an LHM, $\boldsymbol{E}$, $\boldsymbol{H}$ and $\boldsymbol{S}$ form a right-handed triad and $\boldsymbol{S}$ still points in the same direction as the propagation of energy, as in an RHM. Thus, in an LHM, $\boldsymbol{v}_p$ and $\boldsymbol{v}_g$ are of opposite sign and the wave fronts propagate towards the source.

Now let's consider how Snell's law of refraction applies in the case of a NI medium. Recalling that the ratio of the sine functions of the angles of incidence and refraction (to the surface normal) of a wave crossing an interface between two media is equivalent to the ratio of the velocities of the wave in the two media, Snell's Law can be expressed as

$$\frac{\sin\theta_1}{\sin\theta_2} = \frac{v_1}{v_2} = \frac{n_2}{n_1} \tag{12}$$

or, equivalently, as $n_1 \sin\theta_1 = n_2 \sin\theta_2$. A conventional case in which $n_2 > n_1 > 0$ is illustrated in Fig. 1a). In the case of one of the media having negative refractive index, then the refracted wave propagates on the same side of the surface normal as the incident wave. This is illustrated in Fig. 1b) for the case $n_2 = -n_1$, for which $\sin\theta_2 = -\sin\theta_1$ and $\theta_2 = -\theta_1$ due to the odd nature of the sine function. In the next section it will be shown how a planar

slab of NI material can form a focusing device for electromagnetic waves (Veselago, 1968). Not only that, but we will see how a planar slab of negative index material with the property $n_2 = -n_1$ forms a so-called 'perfect' lens in the sense that it overcomes the limitations of conventional optics by focusing all Fourier components of an incident wave including evanescent components that are usually lost to damping (Pendry, 2000).

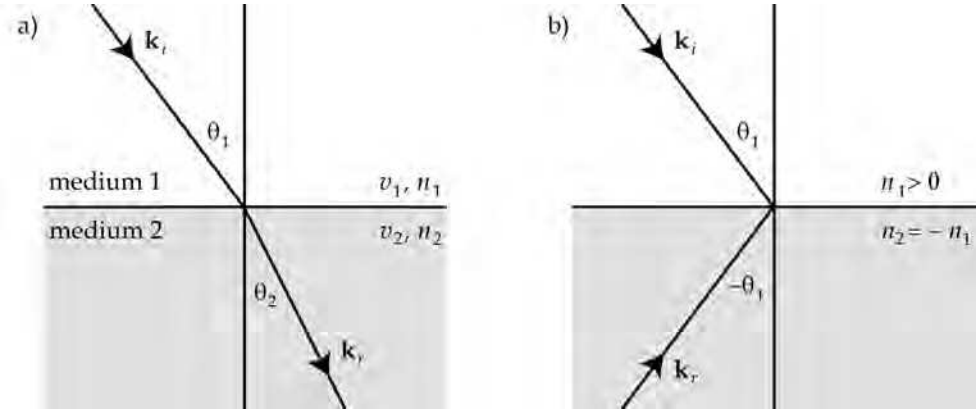

Fig. 1. Snell's Law of Refraction illustrated for a) a conventional case in which $n_2 > n_1 > 0$ and b) the case in which medium 2 has negative refractive index, $n_2 = -n_1$.

2.4 Negative-refractive-index medium as a planar lens

According to classical optics, the resolving power of a conventional optical lens is fundamentally limited in a manner that is related to the wavelength of the light passing through it. This limitation cannot be overcome by improving the quality of the lens. Consider a z-directed electromagnetic wave incident on a conventional lens whose axis is parallel to the z-direction. From Maxwell's equations it can be shown that the wavenumber in the direction of propagation, k_z, is given by

$$k_z = \sqrt{(\omega/c)^2 - k_x^2 - k_y^2}, \qquad (\omega/c)^2 > k_x^2 + k_y^2, \tag{13}$$

for relatively small values of the transverse wavevector $k_x^2 + k_y^2$. In (13), ω is the angular frequency, c the speed, and k_x and k_y are x- and y-directed Fourier components of the electromagnetic wave. The lens operates by correcting the phase of each of the Fourier components of the wave so that they are brought to a focus some distance beyond the lens, producing an image of the source. The condition $(\omega/c)^2 > k_x^2 + k_y^2$ given in (13) provides the restriction on the resolving power of the lens because the transverse wavevector may not exceed a certain maximum magnitude; $k_{\max} = \omega/c$. This means that the best resolution of the lens, Δ, is limited to (cannot be smaller than)

$$\Delta \approx \frac{2\pi}{k_{\max}} = \frac{2\pi c}{\omega} = \lambda \tag{14}$$

where λ is the wavelength.

Some time ago it was shown that a planar slab of NI material has the ability to behave as a lens, bringing propagating light to a focus both within and beyond the slab (Veselago, 1968). This can be shown easily by applying Snell's Law in the manner of Fig. 1b) to two parallel surfaces. As illustrated in Fig. 2, light originating in a medium with refractive index $n_1 > 0$, and from a source located at distance d_1 from the first face of a NI slab with thickness d_2 and negative index $n_2 = -n_1$, is refracted to a focus both *within* the slab (at distance d_1 from the first face) and again on emerging from the slab, at distance $d_2 - d_1$ from the second face.

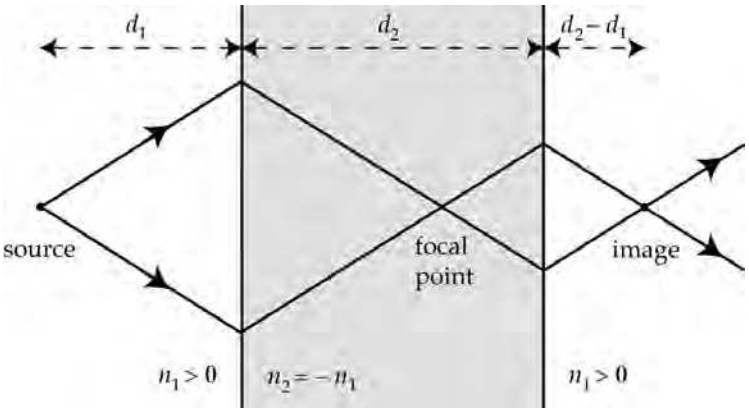

Fig. 2. Light focusing by a planar lens formed from a slab of NI material. The z-direction is from left to right.

More recently, it was pointed out that not only are the propagating components of the light represented by (13) brought to a focus by the lens illustrated in Fig. 2, but so are the evanescent components that are lost to damping in a conventional optical lens (Pendry, 2000). This has led to adoption of the term 'perfect lens' to describe the lens of Fig. 2.

The real wavenumber expressed in (13) represents only propagating waves. Evanescent waves are described by the other inequality $(\omega/c)^2 < k_x^2 + k_y^2$, in other words for relatively large values of $k_x^2 + k_y^2$. Rather than as in (13), k_z is now imaginary, written as

$$k_z = -j\sqrt{k_x^2 + k_y^2 - (\omega/c)^2}, \qquad (\omega/c)^2 < k_x^2 + k_y^2, \tag{15}$$

and the wave is evanescent, decaying exponentially with z. The phase corrective behaviour of a conventional lens works only for the propagating components of the wave represented in (13) because it cannot restore the reduced amplitude of the evanescent components. The focusing mechanism of the planar NI lens is, however, able to cancel the decay of evanescent waves. Surprisingly, evanescent waves emerge from the second face of the lens enhanced in amplitude (Pendry, 2000).

Another important practical feature is exhibited by the perfect lens. Since the condition $n_2 = -n_1$ derives from the relations $\varepsilon_2 = -\varepsilon_1$ and $\mu_2 = -\mu_1$ between the material parameters of the two media, their impedances are perfectly matched; $Z = \sqrt{\mu_1/\varepsilon_1} = \sqrt{\mu_2/\varepsilon_2}$. In other words, there is no reflection loss at the faces of an ideal perfect lens – it is a perfect transmitter. Obviously this is a result of tremendous practical significance.

Now that we have considered some of the fundamental behaviours of an NI material, we move to consider how such a material might be constructed.

3. Dielectric Resonator Composites

3.1 Dielectric resonators for NI metamaterials

Materials composed of especially engineered components that together exhibit properties and behaviours not shown by the individual constituents are often termed metamaterials (Sihvola, 2002). As mentioned in the introduction to this chapter, many experimental demonstrations of NI materials to date have relied upon metallic elements to achieve $\varepsilon < 0$ below the plasma frequency of the metal, and other specially shaped metallic elements to achieve negative permeability $\mu < 0$ due to resonance that is created in or between them in a certain frequency band (Smith et al., 2000; Zhou et al., 2006). In a contrasting approach, the possibility of forming an isotropic DNG metamaterial by collecting together a three-dimensional array of non-conductive, magneto-dielectric spheres has also been proposed (Holloway et al., 2003). In that case, a simple-cubic array of spheres was analyzed and DNG behaviour predicted at frequencies just above those of the Mie resonances for TE and TM mode polarizations, which were made to occur at similar frequencies in order to give $\mathrm{Re}\{\varepsilon\} < 0$ and $\mathrm{Re}\{\mu\} < 0$ in overlapping frequency bands.

Of greatest relevance to this discussion, it has been shown that an array of purely dielectric spheres can be made to exhibit isotropic $\mathrm{Re}\{\mu\} < 0$ (Wheeler et al., 2005). Further, two complementary approaches have been reported, showing that isotropic DNG behaviour can be achieved in a system composed of two interpenetrating lattices of dielectric spheres. In the first design, TE and TM resonances were excited at similar frequencies in spheres with different radius but equal permittivity (Vendik et al., 2006; Jylhä et al., 2006). In the second case, two sets of spheres with the same radius but different permittivity were employed to achieve the same effect (Ahmadi & Mosallaei, 2008). These two schemes were adopted because the fundamental electric resonance in a dielectric sphere naturally occurs at higher frequency than the fundamental magnetic resonance (Bohren & Huffman, 1983). In order to achieve overlapping bands of $\mathrm{Re}\{\varepsilon\} < 0$ and $\mathrm{Re}\{\mu\} < 0$, the resonance frequencies ω_r of the two sphere types must be made to be similar. From the analysis of Mie theory it is found that $\omega_r \propto 1/(a\sqrt{\varepsilon_{r1}})$, where a is the sphere radius and ε_{r1} its relative permittivity. This allows tuning of ω_r by adjusting a and/or ε_{r1}.

3.2 Dielectric resonators

Not only are spherical resonators good candidates for dielectric NI metamaterials, but other shapes, in particular cylinders, have been studied and employed in various microwave applications for some time. A general discussion of the properties of dielectric resonators of various kinds may be found in the text edited by Kajfez & Guillon (1986). A specific example of the use of cylindrical dielectric resonators to provide $\mathrm{Re}\{\mu\} < 0$ in a NI prism was demonstrated recently (Ueda et al., 2007).

3.3 Plane wave scattering by a dielectric sphere

A dielectric sphere in the path of an incident plane electromagnetic wave gives rise to a scattered wave that exhibits an infinite number of resonances due to resonant modes excited

in the sphere. The frequencies at which these resonances occur depend on the permittivity and radius of the sphere, and the wavelength of the incident wave. As mentioned above, these resonances in ε and μ can be exploited to achieve DNG behaviour in a composite metamaterial. In order to design a composite that exhibits DNG behaviour, it is useful to understand the theory of plane wave scattering by a dielectric sphere.

First solved by Gustav Mie (Mie, 1908), a modern description of the theory of plane wave scattering by a sphere has been given by Bohren & Huffman (1983). In the context of designing NI metamaterials by collecting together an array of dielectric spheres, Mie's theory provides a foundation for understanding how the material parameters of the constituents, the particle radius and permittivity and the matrix permittivity, affect the frequencies and bandwidths of the electric and magnetic resonances that lead to $\varepsilon < 0$ and $\mu < 0$. For this reason it is instructive to study the theory, although it should be kept in mind that the development is for an isolated sphere. In the case of a composite in which the spherical inclusions are quite disperse (i.e. the volume fraction is low, around 0.3 or smaller, and the particles are well-separated), predictions of the frequencies of the resonant modes according to Mie theory can be expected to be quite numerically accurate. If the system is not dilute, however, the predictions of Mie theory can provide qualitative guidelines for DNG metamaterials design, but inter-particle interaction effects should be taken into account to achieve numerical accuracy. Here, the main features of Mie theory are outlined. For full details the reader is referred to Bohren & Huffman (1983).

3.3.1 Governing equations and general solution

We begin with the equations that govern a time-harmonic electromagnetic field in a linear, isotropic, homogeneous medium. Both the sphere and the surrounding medium are assumed to have these properties. From Maxwell's equations, the electric and magnetic fields must satisfy the wave equation;

$$(\nabla^2 + k^2)\boldsymbol{E} = 0, \qquad (\nabla^2 + k^2)\boldsymbol{H} = 0, \tag{16}$$

in which $k^2 = \omega^2\varepsilon\mu$. They must also be divergence-free;

$$\nabla \cdot \boldsymbol{E} = 0, \qquad \nabla \cdot \boldsymbol{H} = 0 \tag{17}$$

and are related to each other as follows;

$$\nabla \times \boldsymbol{E} = -j\omega\mu\boldsymbol{H}, \qquad \nabla \times \boldsymbol{H} = j\omega\varepsilon\boldsymbol{E}. \tag{18}$$

The solution proceeds by constructing two vector functions, $\boldsymbol{M}$ and $\boldsymbol{N}$, that both satisfy the vector wave equation and are defined in terms of the same *scalar* function ψ and an arbitrary constant vector $\boldsymbol{c}$. Through these constructions, the problem of finding solutions to the vector field equations (16), (17) and (18) reduces to the simpler problem of solving the scalar wave equation $(\nabla^2 + k^2)\psi = 0$. Later, the vector functions $\boldsymbol{M}$ and $\boldsymbol{N}$ will be employed to express an incident plane wave in terms of an infinite sum of vector spherical harmonics. This facilitates the application of interface conditions at the surface of the scattering sphere and allows the solution to be determined.

Construct the vector function $\boldsymbol{M} = \nabla \times (\boldsymbol{c}\psi)$ for which, by identity, $\nabla \cdot \boldsymbol{M} = 0$. Employing vector identity relations it can be shown that

$$(\nabla^2 + k^2)\boldsymbol{M} = \nabla \times [\boldsymbol{c}(\nabla^2 + k^2)\psi]. \tag{19}$$

This means that $\boldsymbol{M}$ satisfies the vector wave equation if ψ is a solution of the scalar wave equation. Now construct a second vector function $\boldsymbol{N} = \frac{1}{k}\nabla \times \boldsymbol{M}$, that also satisfies the vector wave equation

$$(\nabla^2 + k^2)\boldsymbol{N} = 0 \tag{20}$$

and is also be related to $\boldsymbol{M}$ by $\nabla \times \boldsymbol{N} = k\boldsymbol{M}$. Through these definitions it is seen that $\boldsymbol{M}$ and $\boldsymbol{N}$ exhibit all the required properties of an electromagnetic field;

- Both $\boldsymbol{M}$ and $\boldsymbol{N}$ satisfy the vector wave equation.
- They are divergence free.
- The curl of $\boldsymbol{M}$ is proportional to $\boldsymbol{N}$.
- The curl of $\boldsymbol{N}$ is proportional to $\boldsymbol{M}$.

The solution for plane wave scattering by a sphere will now be obtained by solving the scalar wave equation for ψ, from which the electromagnetic field represented by $\boldsymbol{M}$ and $\boldsymbol{N}$ can be obtained via their definitions in terms of ψ, given above.

Before continuing, note that ψ is often termed a *generating function* for the *vector harmonics* $\boldsymbol{M}$ and $\boldsymbol{N}$, whereas $\boldsymbol{c}$ is termed the *guiding* or *pilot* vector. It is also useful to note that $\boldsymbol{M} = -\boldsymbol{c} \times \nabla\psi$, which implies that $\boldsymbol{M}$ is directed perpendicular to the pilot vector.

The specific choice of pilot vector is guided by the geometry of the particular problem at hand. In the case of plane wave scattering by a sphere centered at the origin of a spherical coordinate system, a natural choice for the pilot vector is the radial vector $\boldsymbol{r}$. Then,

$$\boldsymbol{M} = \nabla \times (\boldsymbol{r}\psi) \tag{21}$$

is everywhere tangential to a spherical surface defined by $|\boldsymbol{r}| = constant$, and ψ is selected to be a solution of the scalar wave equation in spherical polar coordinates. Assuming a particular solution $\psi(r, \theta, \varphi) = R(r)\Theta(\theta)\Phi(\varphi)$, the scalar wave equation in spherical polar coordinates can be separated into three equations;

$$\begin{gathered} \frac{d^2\Phi}{d\varphi^2} + m^2\Phi = 0 \\ \frac{1}{\sin\theta}\frac{d}{d\theta}\left(\sin\theta\frac{d\Theta}{d\theta}\right) + \left[n(n+1) - \frac{m^2}{\sin^2\theta}\right]\Theta = 0 \\ \frac{d}{dr}\left(r^2\frac{dR}{dr}\right) + [k^2r^2 - n(n+1)]R = 0 \end{gathered} \tag{22}$$

where the constants of separation m and n are to be determined by other conditions that ψ must satisfy. The linearly independent solutions for Φ are

$$\Phi_e = \cos m\varphi \quad \text{and} \quad \Phi_o = \sin m\varphi \tag{23}$$

in which the subscripts e and o denote even and odd functions of φ, respectively. Solutions for Θ that are finite at $\theta = 0$ and π are associated Legendre functions of the first kind; $P_n^m(\cos\theta)$ of degree n and order m where $n = m, m+1, \ldots$. When $m = 0$ the $P_n(\cos\theta)$ are the Legendre polynomials. For the dependence on the radial variable r, the solution is obtained by introducing the dimensionless variable $\rho = kr$ and the function $R' = R\sqrt{\rho}$. Then the third of the group of equations (22) becomes

$$\rho\frac{d}{d\rho}\left(\rho\frac{dR'}{d\rho}\right)+\left[\rho^2-\left(n+\frac{1}{2}\right)^2\right]R'=0 \tag{24}$$

with solutions being the Bessel functions of the first and second kinds, J_ν and Y_ν, with half-integer order $\nu = n + 1/2$. The fact that the order is half-integer indicates that the linearly independent solutions of (24) are the *spherical* Bessel functions

$$j_n(\rho)=\sqrt{\frac{\pi}{2\rho}}\,J_{n+1/2}(\rho)\quad\text{and}\quad y_n(\rho)=\sqrt{\frac{\pi}{2\rho}}\,Y_{n+1/2}(\rho). \tag{25}$$

The $j_n(\rho)$ are finite as $\rho \to 0$ whereas the $y_n(\rho)$ are singular as $\rho \to 0$. For example,

$$j_0(\rho)=\frac{\sin\rho}{\rho},\quad j_1(\rho)=\frac{\sin\rho}{\rho^2}-\frac{\cos\rho}{\rho}, \tag{26}$$

$$y_0(\rho)=-\frac{\cos\rho}{\rho}\quad\text{and}\quad y_1(\rho)=-\frac{\cos\rho}{\rho^2}-\frac{\sin\rho}{\rho}. \tag{27}$$

From these first two orders of the spherical Bessel functions, the higher-order functions can be generated by means of recurrence relations. At this point it is useful to define the spherical Bessel functions of the third kind, also known as spherical Hankel functions, that shall be useful in later developments;

$$h_n^{(1)}(\rho)=j_n(\rho)+jy_n(\rho)\quad\text{and}\quad h_n^{(2)}(\rho)=j_n(\rho)-jy_n(\rho). \tag{28}$$

For the reader who is not familiar with the properties of these functions, an excellent resource is the handbook edited by Abramowitz & Stegun (1972).

Having obtained linearly independent solutions to the set of equations (22), we can write down two linearly independent functions that satisfy the scalar wave equation in spherical polar coordinates;

$$\psi_{emn}=z_n(kr)\,P_n^m(\cos\theta)\cos m\varphi\quad\text{and}\quad\psi_{omn}=z_n(kr)\,P_n^m(\cos\theta)\sin m\varphi. \tag{29}$$

In (29), $z_n(kr)$ represents any of the four spherical Bessel functions given in (25) and (28). Any function that satisfies the scalar wave equation in spherical polar coordinates may be expanded as an infinite series in the functions (29), because these functions form a complete set. Write the vector spherical harmonics generated by ψ_{emn} and ψ_{omn} as

$$\boldsymbol{M}_{emn}=\nabla\times(\boldsymbol{r}\psi_{emn}),\quad\boldsymbol{M}_{omn}=\nabla\times(\boldsymbol{r}\psi_{omn}), \tag{30}$$

$$\boldsymbol{N}_{emn}=\frac{1}{k}\nabla\times\boldsymbol{M}_{emn}\quad\text{and}\quad\boldsymbol{N}_{omn}=\frac{1}{k}\nabla\times\boldsymbol{M}_{omn}. \tag{31}$$

Now, any solution of the field equations can be expanded in an infinite series of the functions $\boldsymbol{M}_{emn}$, $\boldsymbol{M}_{omn}$, $\boldsymbol{N}_{emn}$ and $\boldsymbol{N}_{omn}$. This is how the problem of plane wave scattering by a sphere can be solved. Note again that, as a consequence of choosing $\boldsymbol{r}$ as the pilot vector, $\boldsymbol{M}_{emn}$ and $\boldsymbol{M}_{omn}$ are transverse to the radial direction, with only $\hat{\theta}$- and $\hat{\varphi}$-components, whereas $\boldsymbol{N}_{emn}$ and $\boldsymbol{N}_{omn}$ exhibit a radial component as well.

3.3.2 Expansion of a plane wave in vector spherical harmonics

Forming the relationship between an incident plane wave, that is most easily described in a Cartesian coordinate system, and a scatterer whose boundary is a sphere, that is obviously

best described in a spherical coordinate system, is the central issue in the solution of plane wave scattering by a sphere. The development of the previous section, in which it was shown that the vector spherical harmonics $\boldsymbol{M}_{emn}$, $\boldsymbol{M}_{omn}$, $\boldsymbol{N}_{emn}$ and $\boldsymbol{N}_{omn}$ form a complete set that can represent any function that satisfies the scalar wave equation in spherical polar coordinates, will now be employed to represent the plane wave incident on the sphere. In this way, application of the interface conditions at the sphere boundary becomes straightforward.

Consider a plane, x-polarized wave propagating in the z-direction and incident on an arbitrary sphere;

$$\boldsymbol{E}^i = E_0 e^{-jkz}\hat{x} = E_0 e^{-jkr\cos\theta}\hat{x}. \tag{32}$$

Expand (32) in vector spherical harmonics. In general,

$$\boldsymbol{E}^i = \sum_{m=0}^{\infty}\sum_{n=m}^{\infty}\left(B_{emn}\boldsymbol{M}_{emn} + B_{omn}\boldsymbol{M}_{omn} + A_{emn}\boldsymbol{N}_{emn} + A_{omn}\boldsymbol{N}_{omn}\right), \tag{33}$$

but various orthogonality relationships imply that many of these terms are identically zero (Bohren & Huffman, 1983). In fact, the only terms that are non-zero are those with coefficients B_{o1n} and A_{e1n}. Further, the incident field is finite at the origin of the spherical coordinate system, which means that the appropriate spherical Bessel function in the generating functions ψ_{o1n} and ψ_{e1n} is $j_n(kr)$. Indicating the presence of $j_n(kr)$ in the generating functions by superscript (1), $\boldsymbol{E}^i$ can be written

$$\boldsymbol{E}^i = \sum_{n=1}^{\infty}\left(B_{o1n}\boldsymbol{M}_{o1n}^{(1)} + A_{e1n}\boldsymbol{N}_{e1n}^{(1)}\right). \tag{34}$$

To complete the expression of $\boldsymbol{E}^i$ in terms of vector spherical harmonics, it remains to evaluate the coefficients B_{o1n} and A_{e1n}. Evaluation of the appropriate integrals (Bohren & Huffman, 1983) shows that B_{o1n} and A_{e1n} differ only by the factor j. Finally, the desired expansion of the plane wave is found as

$$\boldsymbol{E}^i = \sum_{n=1}^{\infty} E_n\left(\boldsymbol{M}_{o1n}^{(1)} + j\boldsymbol{N}_{e1n}^{(1)}\right) \tag{35}$$

and

$$\boldsymbol{H}^i = -\frac{k}{\omega\mu}\sum_{n=1}^{\infty} E_n\left(\boldsymbol{M}_{e1n}^{(1)} - j\boldsymbol{N}_{o1n}^{(1)}\right) \tag{36}$$

with

$$E_n = E_0(-j)^n\frac{2n+1}{n(n+1)}. \tag{37}$$

$\boldsymbol{H}^i$, (36), was obtained by taking the curl of $\boldsymbol{E}^i$, (35), according to (18).

3.3.3 The scattered field and scattering coefficients

Assume the scatterer to be a homogeneous, isotropic sphere with radius a, permittivity ε_1 and permeability μ_1. In order to apply interface conditions at the surface of the sphere, it is

necessary to express the electromagnetic field internal to the sphere, and the electromagnetic field scattered by it, in terms of vector spherical harmonics.

As in the case of the incident field, the field internal to the sphere is finite at the origin of the spherical coordinate system and, therefore, $j_n(kr)$ is the appropriate spherical Bessel function in the generating functions ψ_{o1n} and ψ_{e1n}. Denoting the fields internal to the sphere by the superscript int,

$$\boldsymbol{E}^{int} = \sum_{n=1}^{\infty} E_n \left(c_n \boldsymbol{M}_{o1n}^{(1)} + j d_n \boldsymbol{N}_{e1n}^{(1)} \right) \tag{38}$$

and

$$\boldsymbol{H}^{int} = -\frac{k_1}{\omega \mu_1} \sum_{n=1}^{\infty} E_n \left(d_n \boldsymbol{M}_{e1n}^{(1)} - j c_n \boldsymbol{N}_{o1n}^{(1)} \right) \tag{39}$$

where the wavenumber inside the sphere is given by $k_1^2 = \omega^2 \varepsilon_1 \mu_1$.

The scattered field external to the sphere, denoted by the superscript s, is appropriately expressed in terms of the spherical Hankel functions of the first kind $h_n^{(1)}$. This is the correct choice because both j_n and y_n are well-behaved outside the sphere, and at large distances $h_n^{(1)}$ represents an outgoing spherical wave according to

$$h_n^{(1)}(kr) \sim -j^n \frac{e^{-jkr}}{jkr}, \quad kr \gg n^2. \tag{40}$$

Then,

$$\boldsymbol{E}^{s} = -\sum_{n=1}^{\infty} E_n \left(b_n \boldsymbol{M}_{o1n}^{(3)} + j a_n \boldsymbol{N}_{e1n}^{(3)} \right) \tag{41}$$

and

$$\boldsymbol{H}^{s} = \frac{k}{\omega \mu} \sum_{n=1}^{\infty} E_n \left(a_n \boldsymbol{M}_{e1n}^{(3)} - j b_n \boldsymbol{N}_{o1n}^{(3)} \right) \tag{42}$$

in which the superscript (3) indicates that the radial dependence of the generating functions is specified by $h_n^{(1)}$. With the incident, internal and scattered fields now all expressed in terms of vector spherical harmonics, in (35) through (42), it is now possible to apply interface conditions and determine the coefficients a_n, b_n, c_n and d_n.

Continuity of the tangential components of $\boldsymbol{E}$ and $\boldsymbol{H}$ at the sphere boundary may be expressed

$$\left(\boldsymbol{E}^{i} + \boldsymbol{E}^{s} - \boldsymbol{E}^{int} \right) \times \hat{r} = \left(\boldsymbol{H}^{i} + \boldsymbol{H}^{s} - \boldsymbol{H}^{int} \right) \times \hat{r} = 0. \tag{43}$$

Applying these conditions to the field expansions leads to a system of linear equations that may be solved readily for the coefficients a_n, b_n, c_n and d_n. Here, only a_n and b_n are given explicitly since they are important for the application of interest in this chapter; determining the bulk response of a composite material formed from a mixture of spherical scatterers embedded in a supporting matrix. Similar expressions exist for c_n and d_n (Bohren & Huffman, 1983). To express the coefficients a_n and b_n compactly it is convenient to

introduce i) the dimensionless size parameter $\alpha = ka = 2\pi na/\lambda$, in which n is the refractive index of the medium external to the sphere and ii) the relative refractive index defined as the ratio of that in the sphere to that external to the sphere; $N = n_1/n$. After some manipulation,

$$a_n = \frac{\mu N^2 j_n(N\alpha)[\alpha j_n(\alpha)]' - \mu_1 j_n(\alpha)[N\alpha j_n(N\alpha)]'}{\mu N^2 j_n(N\alpha)\left[\alpha h_n^{(1)}(\alpha)\right]' - \mu_1 h_n^{(1)}(\alpha)[N\alpha j_n(N\alpha)]'} \tag{44}$$

and

$$b_n = \frac{\mu_1 j_n(N\alpha)[\alpha j_n(\alpha)]' - \mu j_n(\alpha)[N\alpha j_n(N\alpha)]'}{\mu_1 j_n(N\alpha)\left[\alpha h_n^{(1)}(\alpha)\right]' - \mu h_n^{(1)}(\alpha)[N\alpha j_n(N\alpha)]'}. \tag{45}$$

In (44) and (45) the prime denotes that the derivative with respect to the argument of the Bessel function should be taken. This pair of equations is also commonly written in terms of the Riccati-Bessel functions, $\rho z_n(\rho)$, where $z_n(\rho)$ represents any of the four spherical Bessel functions given in (25) and (28).

In general, the scattered field is a superposition of normal modes. Due to the forms of (44) and (45), however, there are conditions under which one particular mode may dominate, when the denominator of either (44) or (45) is very small. These are the conditions that lead to resonance in either the bulk permittivity or permeability of a composite filled with identical dielectric spheres and, therefore, to negative bulk permittivity and permeability in a band above the resonant frequency.

The a_n mode dominates for a particular n when the frequency or particle radius is such that

$$\frac{\left[\alpha h_n^{(1)}(\alpha)\right]'}{h_n^{(1)}(\alpha)} = \frac{\mu_1[N\alpha j_n(N\alpha)]'}{\mu N^2 j_n(N\alpha)} = \frac{\varepsilon}{\varepsilon_1}\frac{[N\alpha j_n(N\alpha)]'}{j_n(N\alpha)}. \tag{46}$$

Likewise, the b_n mode dominates for

$$\frac{\left[\alpha h_n^{(1)}(\alpha)\right]'}{h_n^{(1)}(\alpha)} = \frac{\mu}{\mu_1}\frac{[N\alpha j_n(N\alpha)]'}{j_n(N\alpha)} \tag{47}$$

Note that these two expressions differ only in the ratios $\varepsilon/\varepsilon_1$ and μ/μ_1. Dominance of a_n implies that $\boldsymbol{E}^s \propto \boldsymbol{N}_{\mathrm{e}1n}^{(3)}$ and $\boldsymbol{H}^s \propto \boldsymbol{M}_{\mathrm{e}1n}^{(3)}$. These are transverse magnetic (TM) modes in which there is no radial component of $\boldsymbol{H}^s$ since the $\boldsymbol{M}_{\mathrm{e}1n}$ **and** $\boldsymbol{M}_{\mathrm{o}1n}$ have only $\hat{\theta}$- and $\hat{\varphi}$-components. Similarly, dominance of b_n implies that $\boldsymbol{E}^s \propto \boldsymbol{M}_{\mathrm{o}1n}^{(3)}$ and $\boldsymbol{H}^s \propto \boldsymbol{N}_{\mathrm{o}1n}^{(3)}$. When b_n dominates, the modes are transverse electric (TE), for which there is no radial component of $\boldsymbol{E}^s$. Several texts (Stratton, 1941; Bohren & Huffman, 1983) reproduce Mie's original diagrams (Mie, 1908) showing the electric field distribution on a spherical surface with radius greater than a, for the first few TM and TE modes. Also note that for any particular order n of the spherical Bessel functions in (46) and (47) there are an infinite number of resonances as a function of the size parameter α (Roll & Schweiger, 2000).

3.4 Resonators in a composite

One way in which the results of the previous section can be employed to predict the bulk permittivity and permeability of a composite containing dielectric spheres is by treating the composite as an effective medium. In order to treat the composite in this way, the wavelength of the incident field in the effective medium must be significantly larger than

the particle diameter or other significant length scale. For example, effective permittivity and permeability of a simple-cubic lattice of dielectric spheres can be obtained via a modified Maxwell-Garnett relation provided that the wavelength of the incident wave is significantly greater than the lattice constant of the cubic lattice (Lewin, 1947; Holloway et al., 2003).

If the wavelength within the particles is also long, then the response is quasi-static and the electric and magnetic fields are decoupled. The effective permittivity and permeability of the mixture may each be described by the Maxwell-Garnett formula, or by other formulas (Sihvola, 1999). If, on the other hand, the wavelength within the particles is similar to the particle diameter then the dynamic Maxwell equations apply, within the particle, and the electric and magnetic fields are coupled. This is the problem solved by Lewin (1947) for a simple-cubic array of spheres embedded in a host medium. The details of the solution are not repeated here but the result may be summarized as follows.

For an array of homogeneous spheres arranged on the nodes of a simple-cubic lattice and embedded in a matrix with relative permittivity ε_r and permeability μ_r the relative effective permittivity ε_{re} and permeability μ_{re} of the mixture are given by expressions that are *formally* similar to the Maxwell-Garnett mixture formula;

$$\varepsilon_{re} = \varepsilon_r \left(1 + \frac{3f}{\frac{\varepsilon_{rp} + 2\varepsilon_r}{\varepsilon_{rp} - \varepsilon_r} - f} \right) \quad \text{and} \quad \mu_{re} = \mu_r \left(1 + \frac{3f}{\frac{\mu_{rp} + 2\mu_r}{\mu_{rp} - \mu_r} - f} \right), \tag{48}$$

where f is the volume fraction of the spherical inclusions. In the quasi-static regime, ε_{rp} and μ_{rp} are none other than the particle parameters ε_{r1} and μ_{r1}, and equations (48) reduce directly to the Maxwell-Garnett formula. In the case in which the wavelength within the particle, λ_1, is similar to the particle diameter $2a$, however, the effective permittivity and permeability of the particles ε_{rp} and μ_{rp} are given by (Lewin, 1947; Holloway et al., 2003)

$$\varepsilon_{rp} = F(\vartheta)\varepsilon_{r1} \quad \text{and} \quad \mu_{rp} = F(\vartheta)\mu_{r1}. \tag{49}$$

The function $F(\vartheta)$ that represents the coupling of the electric and magnetic fields is given by

$$F(\vartheta) = \frac{2(\sin\vartheta - \vartheta\cos\vartheta)}{(\vartheta^2 - 1)\sin\vartheta + \vartheta\cos\vartheta}, \tag{50}$$

where $\vartheta = k_1 a$ and k_1 is the wavenumber inside the sphere, given by $k_1^2 = \omega^2\varepsilon_1\mu_1$. The possibility of resonant behaviour arises through the form of $F(\vartheta)$ which represents the coupling between the electric and magnetic fields in the system. $F(\vartheta)$ arises from Mie theory under the approximation that the dielectric spheres act as non-interacting dipole resonators. Under this approximation, higher-order multipole modes are neglected. For this reason, (48) and (49) represent an approximation that is strictly valid only for relatively small values of volume fraction; $f \leq 0.3$. When f increases, inter-particle interaction effects may not be neglected. For example, multipolar inter-particle interaction effects of poles of order up to 2^7 among spherical particles arranged on the nodes of a simple-cubic lattice are described by the analytic formula derived by McKenzie et al. (1977). Instead of (48) the inclusion of poles of order up to 2^7 gives lengthier expressions (Liu & Bowler, 2009).

Considering (48) it can be seen that ε_{re} and μ_{re} are at resonance when

$$\varepsilon_{rp}^{\text{res}} = -\varepsilon_r \left(\frac{2+f}{1-f}\right) \quad \text{and} \quad \mu_{rp}^{\text{res}} = -\mu_r \left(\frac{2+f}{1-f}\right). \tag{51}$$

These relations define the effective permittivity or permeability of the particle that is needed to achieve resonance in ε_{re} and μ_{re}. Note that $\varepsilon_{rp}^{\text{res}}$ and μ_{rp}^{res} are negative. From relations (49) and by consideration of the behaviour of function $F(\vartheta)$ it is possible to determine how to engineer ε_{rp} and μ_{rp} to achieve resonance and, therefore, negative bulk permittivity and permeability of the composite; $\varepsilon_{re} < 0$ and $\mu_{re} < 0$ for a band of frequencies just above the resonance frequency.

In Fig. 3, $F(\vartheta)$ is plotted as a function of ϑ and a pattern of quasi-periodic singularities is revealed. As described in section 3.3.3, any one of the modes predicted by Mie theory dominates, for a particular order n of the spherical Bessel functions, when the frequency or particle radius is such that (46) and (47) are satisfied. Also recall that for any particular n there is an infinite number of resonances whose frequencies depend on the size parameter ka (Roll & Schweiger, 2000). These resonances give rise to the pattern of singularities (an infinite number) shown in Fig. 3, despite the fact that $F(\vartheta)$ represents only a dipolar approximation to the full Mie theory. Note that the bandwidth of the resonance decreases as ϑ increases.

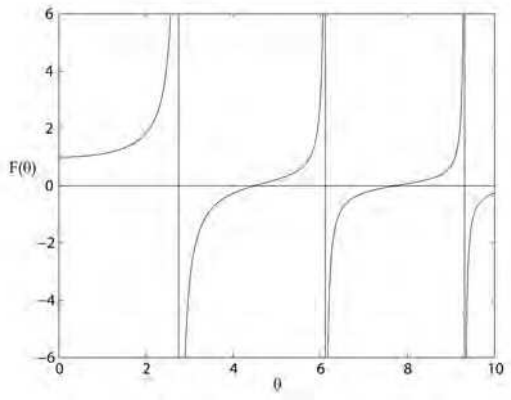

Fig. 3. Functional behaviour of $F(\vartheta)$, equation (50).

In example calculations, Holloway et al. (2003) showed that bands of negative ε and μ can be made to overlap perfectly when $\varepsilon/\varepsilon_1 = \mu/\mu_1$. Elsewhere, it has been discussed that composites formed with identical non-magnetic particles with large ε_1 (i.e. $\varepsilon/\varepsilon_1 \ll \mu/\mu_1$) show a lowest-order resonance in bulk permittivity at a frequency much higher than that in permeability (Jylhä et al., 2006; Vendik et al., 2006; Wheeler et al., 2006; Ahmadi & Mosallaei, 2008). These observations make sense in the light of equations (46) and (47), which embody the full solution to plane wave scattering by a dielectric sphere, and (48) which represents the effective properties of a composite medium based on a dipole approximation of the field scattered by spheres arranged on the nodes of a simple-cubic lattice.

Many experimental demonstrations of NI materials have relied upon metallic elements to achieve negative permittivity $\text{Re}\{\varepsilon\} < 0$ below the plasma frequency of the metal, and other specially shaped metallic elements to achieve negative permeability $\text{Re}\{\mu\} < 0$ due to resonance that is created in or between them in a certain frequency band (Smith et al., 2000; Zhou et al., 2006). In other experimental work, dielectric resonators have been used to

achieve $\mathrm{Re}\{\mu\} < 0$ but not $\mathrm{Re}\{\varepsilon\} < 0$ (Ueda et al., 2007; Cai et al., 2008). Negative phase velocity was demonstrated in an array of magnetodielectric (YIG) spheres (Baker-Jarvis et al., 2006).
It has also been shown experimentally that both periodic and random arrays of dielectric cylinders can compose a metamaterial with DNG properties (Peng et al., 2007). Most recently a waveguide filter has been constructed using a DNG slab formed from two interpenetrating lattices of dielectric spheres with different radius, one to support $\mathrm{Re}\{\mu\} < 0$ and the other $\mathrm{Re}\{\varepsilon\} < 0$ (Siakavara & Damianidis, 2009). This arrangement was analyzed theoretically by Ahmadi & Mosallaei (2008).

4. Selected Applications

4.1 Transmission lines

The application of left-handedness in transmission lines has been a subject of intense research in recent years. One common configuration is the employment of a periodic, linear array of metallic elements to achieve $\varepsilon < 0$ and $\mu < 0$, although the elements themselves are of a wide variety of shapes and designs. A recent summary of this field is given in the text by Marqués et al. (2008).

4.2 Patch antennas

Patch antenna sensors have recently been designed for near-field material property characterization measurements (Zucchelli et al., 2008; Li & Bowler, 2009). Permittivity of a test-piece can be extracted from a measured shift in the resonant frequency of a patch sensor as it is brought near to the test-piece. Or, anomalies in a dielectric material can be detected by the shift in resonant frequency of the sensor. Sensor sensitivity may be defined as the magnitude of the shift in resonant frequency per unit change in test-piece relative permittivity. In both recent works in this area it has been shown that the sensor sensitivity can be improved by reducing the permittivity of the sensor substrate, which forms an insulating layer between the ground plane and resonating patch. Both the permittivity and thickness of the sensor substrate are the primary factors determining the sensor sensitivity but, in order to guarantee the resonant state and penetration depth of the sensor, the substrate thickness is confined to a small range (Bhartia et al., 2001). Employing a negative permittivity substrate, on the other hand, can provide much better sensitivity compared with that of a sensor with a conventional substrate. The sensitivity variation for substrates with various permittivity values is shown in Fig. 4 as a function of the permittivity of the core (second layer) in a three-layer dielectric test-piece, calculated according to an analytic formula (Bernhard & Tousignant, 1999). It can be seen that sensitivity is dramatically enhanced as substrate permittivity becomes negative.

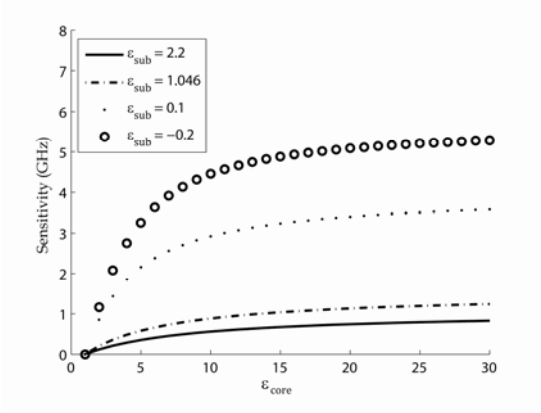

Fig. 4. Change in resonant frequency (sensitivity) of a 10 mm x 10 mm half-wave patch sensor as a function of second-layer (half-space core) permittivity in a coated half-space test-piece, for various values of sensor substrate permittivity. Thickness of the test-piece coating adjacent to the sensor is 0.9 mm and its relative permittivity is 4. Thickness of the sensor substrate is 1.1 mm. Sensitivity values are plotted relative to the resonant frequency for $\varepsilon_{\text{core}} = 1$.

4.3 Superlens

A planar lens fabricated from a metamaterial that exhibits NI behaviour at microwave frequencies can be used to focus the electromagnetic wave emitted by a microwave sensor such as a transmitting monopole or horn antenna. As described in section 2.4 above, this kind of lens can achieve sub-wavelength resolution via the so-called 'perfect lens' effect (Veselago, 1968; Pendry, 2000).

Practically speaking, such a lens can be used to combine the advantages of near-field and far-field microwave nondestructive evaluation (NDE) methods by operating at stand-off distances typical for the far-field mode, on the order of tens of centimeters, yet achieving probe size and spatial resolution typical of the near-field mode, on the order of millimeters (Shreiber et al., 2008). For example, the method is not significantly sensitive to changes in the probe standoff distance, when compared to conventional near-field methods in microwave NDE.

A NI-lens-based NDE system operating at 3.65 GHz, with 8.2-cm wavelength, has been shown to detect successfully a 0.037 wavelength (3 mm) cylindrical void in a fiberglass sample at a distance approximating far field (Shreiber et al., 2008). The work employed a NI lens formed from an array of thin metallic wires, to achieve negative permittivity, coupled with an array of metallic split-ring resonators, designed to provide negative permeability. This type of NI lens suffers from significant losses due to the metallic elements employed in fabricating the lens, requiring amplification of the signal and use of a pick-up monopole between the lens and sample for adequate signal detection.

The alternative approach discussed in this chapter, of employing a low-loss, purely dielectric metamaterial lens formed from an array of dielectric resonators embedded in a supporting matrix, offers several advantages over a metallic metamaterial lens. Compared with the lens reported by Shreiber et al. (2008), a purely dielectric lens is expected to exhibit

significantly better transmission properties, enabling sub-wavelength resolution for defect detection without the need for signal amplification or use of an additional pick-up sensor. In this way the measurement system can be simplified, the cost reduced and performance improved.

5. Conclusion

To conclude, some key points related to purely dielectric NI metamaterials are emphasized. One advantage of non-metallic DNG materials is improved efficiency due to elimination of metallic loss. In addition, the DNG behaviour does not rely on interparticle interactions, or interactions between unit cells, contrasting with periodic material structures that exhibit DNG behaviour, because the collective response of a metamaterial composed of dielectric resonators arises fundamentally from the properties of each individual resonator. Following from this point, periodic arrangement of the particles is not necessary for DNG behaviour in the dielectric metamaterial system. This suggests that it should be possible to fabricate NI materials using a system of randomly-distributed dielectric particles embedded in a supporting matrix. For microwave applications, smaller particles than those reported by Siakavara & Damianidis (2009) (approximately 1 mm diameter) could be utilized if the particle permittivity is increased, according to $\omega_r \propto 1/(a\sqrt{\varepsilon_{r1}})$. Such a material would be relatively simple to fabricate compared with NI materials that rely on periodicity in their structure. The DNG bandwidth can be increased by moving the resonating elements closer together, because this increases the coupling between them, reducing the quality-factor of the resonances in $\boldsymbol{\varepsilon}$ and $\boldsymbol{\mu}$.

6. Acknowledgment

The author thanks Yang Li and Jin Liu for researching some information that appears in this chapter and for assisting with some of the figures.

7. References

Abramowitz, M. & Stegun, I. A. (Eds.), (1972). *Handbook of Mathematical Functions with Formulas, Graphs, and Mathematical Tables,* Dover, ISBN 486612724, New York.

Ahmadi, A. & Mosallaei, H. (2008). Physical configuration and performance modeling of all-dielectric metamaterials. *Phys. Rev. B,* Vol. 77, Art. No. 045104.

Baker-Jarvis, J.; Janezic, M. D.; Love, D.; Wallis, T. M.; Holloway, C. L. & Kabos, P. (2006). Phase velocity in resonant structures. *IEEE Trans. Magnetics.* Vol. 42, No. 10, 3344-3346.

Bernhard, J. T. & Tousignant, C. J. (1999). Resonant frequencies of rectangular microstrip antennas with flush and spaced dielectric superstrates. *IEEE Trans. Antennas Propagat.*, Vol. 47, No. 2, 302-308.

Bhartia, P.; Bahl, I.; Garg, R. & Ittibipoon, A. (2001). *Microstrip Antenna Design Handbook,* Artech House, ISBN 0890065136, Boston.

Bohren, C. F. & Huffman D. R. (1983). *Absorption and Scattering of Light by Small Particles,* Wiley, ISBN 047105772X, New York.

Cai, X.; Zhu, R. & Hu, G. (2008). Experimental study for metamaterials based on dielectric resonators and wire frame. *Metamaterials*. Vol. 2, 220-226.

Caloz, C.; Chang, C.-C. & Itoh, T. (2001). Full-wave verification of the fundamental properties of left-handed materials in waveguide configurations. *J. Appl. Phys.,* Vol. 90, No. 11, 5483-5486.

Holloway, C. L.; Kuester, E. F.; Baker-Jarvis, J. & Kabos, P. (2003). A double negative (DNG) composite medium composed of magnetodielectric spherical particles embedded in a matrix. *IEEE Trans. Antennas Propagat.,* Vol. 51, No. 10, 2596-2603.

Jylhä, L.; Kolmakov, I.; Maslovski, S. & Tretyakov, S. (2006). Modeling of isotropic backward-wave materials composed of resonant spheres. *J. Appl. Phys.,* Vol. 99, Art. No. 043102.

Kajfez, D. & Guillon, P. (Eds.), (1986). *Dielectric Resonators,* Artech House, ISBN 0890062013, Boston.

Lewin, L. (1947). The electrical constants of a material loaded with spherical particles. *Proc. Inst. Elec. Eng.*, Vol. 94, No. 12, 65-68.

Li, Y. & Bowler, N. (2009). Design of patch sensors for microwave nondestructive evaluation of aircraft radomes. *Proceedings of the 14th International Workshop on Electromagnetic Nondestructive Evaluation (ENDE),* Dayton OH, July 2009, Elsevier, Amsterdam, submitted.

Liu, J. & Bowler, N. (2009). Analysis of bandwidth and losses in non-metallic double-negative (DNG) metamaterials. *IEEE Trans. Antennas Propag.*, submitted.

Marqués, R.; Martín, F. & Sorolla, M. (2008). *Metamaterials with Negative Parameters : Theory, Design, and Microwave Applications,* Wiley, ISBN 9780471745822, New York.

McKenzie, D. R. & McPhedran, R. C. (1977). Exact modeling of cubic lattice permittivity and conductivity. *Nature,* Vol. 265, Issue 5590, 128-129.

Mie, G. (1908). Contributions on the optics of turbid media, particularly colloidal metal solutions. *Annalen der Physik,* Series IV, Vol. 25, No. 3, 377-445.

Pendry, J. B. (2000). Negative refraction makes a perfect lens. *Phys. Rev. Lett.,* Vol. 85, No. 18, 3966-3969.

Peng, L.; Ran, L.; Chen, H.; Zhang, H.; Kong, J. A. & Grzegorczyk, M. (2007). Experimental observation of left-handed behavior in an array of standard dielectric resonators. *Phys. Rev. Lett.*, Vol. 98, Art. No. 157403.

Roll, G. & Schweiger, G. (2000). Geometrical optics model of Mie resonances. *J. Opt. Soc. Am. A*, Vol. 17, No. 7, 1301-1311.

Shreiber, D.; Gupta, M. & Cravey, R. (2008). Microwave nondestructive evaluation of dielectric materials with a metamaterial lens. *Sensors and Actuators A,* Vol. 144, 48-55.

Siakavara, K. & Damianidis, C. (2009). Microwave filtering in waveguides loaded with artificial single or double negative materials realized with dielectric spherical particles in resonance. *Progress in Electromagnetics Res.,* Vol. 95, 103-120.

Sihvola, A. (1999). *Electromagnetic Mixing Formulas and Applications*. The Institution of Electrical Engineers, ISBN 0852967721, London.

Sihvola, A. (2002). Electromagnetic emergence in metamaterials. Deconstruction of terminology of complex media, In: *Advances in Electromagnetics of Complex Media and Metamaterials,* Zouhdi, S. ; Sihvola, A. & Arsalane, M. (Eds.), 3-18, Kluwer, ISBN 1402011016, Boston.

Smith, D. R.; Padilla, Willie J.; Vier, D. C.; Nemat-Nasser, S. C. & Schultz, S. (2000). Composite medium with simultaneously negative permeability and permittivity. *Phys. Rev. Lett.*, Vol. 84, No. 18, 4184-4187.

Stratton, J. A. (1941). *Electromagnetic Theory*. McGraw-Hill, New York.

Ueda, T.; Lai, A. & Itoh, T. (2007). Demonstration of negative refraction in a cutoff parallel-plate waveguide loaded with 2-D square lattice of dielectric resonators. *IEEE Trans. Microwave Theory Tech.* Vol. 55, No. 6, 1280-1287.

Vendik, I.; Vendik, O.; Kolmakov, I. & Odit, M. (2006). Modelling of isotropic double negative media for microwave applications. *Opto-Electronics Rev.,* Vol. 14, No. 3, 179-186.

Veselago, V. G. (1968). Electrodynamics of substances with simultanesouly negative values of sigma and mu. *Sov. Phys. Usp.,* Vol. 10, 509-514.

Wheeler, M. S.; Aitchison, J. S. & Mojahedi, M. (2005). Three-dimensional array of dielectric spheres with an isotropic negative permeability at infrared frequencies. *Phys. Rev. B,* Vol. 72, Art. No. 193103.

Wheeler, M. S.; Aitchison, J. S. & Mojahedi, M. (2006). Coated nonmagnetic spheres with a negative index of refraction at infrared frequencies. *Phys. Rev. B,* Vol. 73, Art. No. 045105.

Zhang, Y. & Mascarenhas, A. (2007). Negative refraction of electromagnetic and electronic waves in uniform media, In: *Physics of Negative Refraction and Negative Index Materials : Optical and Electronic Aspects and Diversified Approaches,* Krowne, C. M. & Zhang, Y. (Eds.), 1-18, Springer, ISBN 9783540721314, New York.

Zhou, J.; Koschny, T.; Zhang, L.; Tuttle G. & Soukoulis, C. M. (2006). Experimental demonstration of negative index of refraction. *Appl. Phys. Lett.*, Vol. 88, Art. No. 221103.

Ziolkowski, R. W. & Heyman, E. (2001). Wave propagation in media having negative permittivity and permeability. *Phys. Rev. E*, Vol. 64, Art. No. 056625.

Zucchelli, A.; Chimenti, M. & Bozzi, E. (2008). Application of a coaxial-fed patch to microwave non-destructive porosity measurements in low-loss dielectrics. *Progress in Electromagn. Res.*, Vol. 5, 1-14.

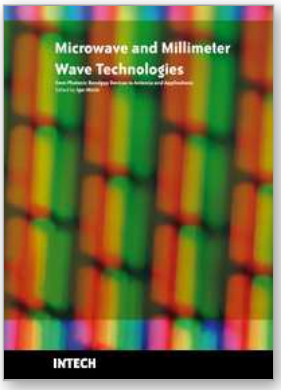

Microwave and Millimeter Wave Technologies from Photonic Bandgap Devices to Antenna and Applications

Edited by Igor Minin

ISBN 978-953-7619-66-4
Hard cover, 468 pages
Publisher InTech
Published online 01, March, 2010
Published in print edition March, 2010

The book deals with modern developments in microwave and millimeter wave technologies, presenting a wide selection of different topics within this interesting area. From a description of the evolution of technological processes for the design of passive functions in milimetre-wave frequency range, to different applications and different materials evaluation, the book offers an extensive view of the current trends in the field. Hopefully the book will attract more interest in microwave and millimeter wave technologies and simulate new ideas on this fascinating subject.

How to reference

In order to correctly reference this scholarly work, feel free to copy and paste the following:

Nicola Bowler (2010). Negative Refractive Index Composite Metamaterials for Microwave Technology, Microwave and Millimeter Wave Technologies from Photonic Bandgap Devices to Antenna and Applications, Igor Minin (Ed.), ISBN: 978-953-7619-66-4, InTech, Available from: http://www.intechopen.com/books/microwave-and-millimeter-wave-technologies-from-photonic-bandgap-devices-to-antenna-and-applications/negative-refractive-index-composite-metamaterials-for-microwave-technology

INTECH
open science | open minds

InTech Europe
University Campus STeP Ri
Slavka Krautzeka 83/A
51000 Rijeka, Croatia
Phone: +385 (51) 770 447
Fax: +385 (51) 686 166
www.intechopen.com

InTech China
Unit 405, Office Block, Hotel Equatorial Shanghai
No.65, Yan An Road (West), Shanghai, 200040, China
中国上海市延安西路65号上海国际贵都大饭店办公楼405单元
Phone: +86-21-62489820
Fax: +86-21-62489821